Impedance Analysis of Polymer Electrolyte Membrane Fuel cell

K. Sankar Naik

A Thesis Submitted to
Indian Institute of Technology Hyderabad
In Partial Fulfillment of the Requirements for
The Degree of Master of Technology

भारतीय प्रौद्योगिकी संस्थान हैदराबाद
Indian Institute of Technology Hyderabad

Department of Chemical Engineering

June 2018

Declaration

I declare that this written submission represents my ideas in my own words, and where ideas or words of others have been included, I have adequately cited and referenced the original sources. I also declare that I have adhered to all principles of academic honesty and integrity and have not misrepresented or fabricated or falsified any idea/data/fact/source in my submission. I understand that any violation of the above will be a cause for disciplinary action by the Institute and can also evoke penal action from the sources that have thus not been properly cited, or from whom proper permission has not been taken when needed.

K. Sankar Naik

(Signature)
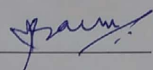
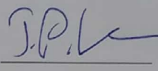KURRA SANKAR NAIK

(Student Name)

CH16MTECH11010

(Roll No.)

Approval Sheet

This Thesis entitled 'Impedance Analysis of Polymer Electrolyte Membrane Fuel cell' by K.Shankar Naik is approved for the degree of Master of Technology from IIT Hyderabad

(Dr.Parag D Pawar) Examiner
Dept. of Chem Eng
IITH

(Dr.Praveen Meduri) Examiner
Dept. Chem Eng
IITH

(Dr.Phanindra Varma Jampana) Adviser
Dept. of Chem Eng
IITH

(Dr. Vinod Janardhanan) Chairman
Dept. of Chem Eng
IITH

Acknowledgements

I would like to express my very great appreciation to Dr. Phanindra Varma Jampana for his valuable and constructive suggestions during the planning and development of this research work.My grateful thanks are also extended to Mr.V. Santhosh Kumar, Mr. V. Goutham Polishetty and K. Koteswara rao and friends.

Finally, I wish to thank my parents for their support and encouragement throughout my study.

Dedication

Dedication to my family

Abstract

Electrochemical Impedance Spectroscopy can be used as a diagnostic tool for fuel cells. In this thesis, a model based impedance analysis of Polymer Electrolyte Membrane Fuel cells is given. The impedance of Cathode Gas Diffusion Layer (GDL) and Cathod Catalyst Layer (CCL) is obtained using physical models from existing literature. The change in the oxygen concentraion at the GDL | CCL interface with respect to a perturbation in the current density is obtained from existing models and shown numerically. Similarly, the change in the activation overpotential at the CCL | membrane interface with respect to a perturbation in the current is again calculated from existing models and calculated numerically.

Contents

Chapter 1

Introduction

1.1 Significance of Fuel cells

Fuel cell is a device which converts chemical energy into electrical energy using electrochemical reactions. Fuel cells have zero emissions and hence are very attractive for transportation and industrial applications. The Fuel cell was invented by William Groves in 1839. There exist many different type of fuel cells as of today.

- Polymer Electrolyte Membrane Fuel cell.

- Solid Oxide fuel cell

- Molten carbon fuel cell

- Alkaline Fuel cell

- Phosphoric Acid fuel cell

In transport applications, Polymer Electrolyte Membrane Fuel cells have high efficiency compared to internal combustion engines [1]. PEMFCs have been used in light weight vehicles and effectively in small scale for buses and forklifts.

1.2 Operation Principle of PEMFC

Fuel cell converts the chemical potential energy of reactants into electrical energy. As in any electrochemical cell, the chemical reaction is split into two half reactions involving flow of electrons and

protons. In Polymer electrolyte membrane fuel cell the two half chemical reactions are divided by a Nafion Membrane which conducts protons but does not allow electrons and gases to pass. Hydrogen and Oxygen supplied to the anode and cathode respectively.

At anode the Hydrogen Oxidation Reaction (HOR) takes place,

$$H_2 \longleftrightarrow 2H^+ + 2e^- \tag{1.1}$$

while at cathode the Oxygen Reduction Reaction (ORR) occurs.

$$O_2 + 4H^+ + 4e^- \longleftrightarrow 2H_2O \tag{1.2}$$

The difference in the chemical potential of reactants is converted to difference in electrical potential when the two half chemical reactions are combined. The theoretical cell potential of PEMFC is 1.23 V. This value can be calcuated using the following expression.

$$E_{cell} = -\frac{\Delta G}{nF} \tag{1.3}$$

Here ΔG is the change in Gibbs free energy of the overall reaction, $n = 4$ is number of electron exchanged and ΔG is the change in Gibbs Free energy for the reaction $2H_2 + O_2 \rightarrow 2H_2 0$ and F is the Faraday's constant.

Polymer electrolyte membrane fuel cell is made of five layers and f low channels with supportive plates as shown in Figure 1.1. The five layers are collectively called as the Membrane Electrode Assembly(MEA). The center layer of MEA is the membrane surrounded by the anode and cathode on either side. Each electrode consists of catalyst and gas diffusion layers. The catalyst layer is porous and consists of carbon supported platinum particles and the ionomer (Nafion). The triple phase boundary between the carbon phase, ionomer and the gas pores is the active area of the cell and the site of electrode half reactions.

Multiple MEAs are stacked together in series to increase voltage and increase the space efficiency. Each MEA stack is covered by bipolar plates on each side with flow channels for hydrogen flow into the anode and oxygen or air into cathode side. Sealed coolant channels are also contained in the bipolar plate for heat rejection. Each cell is sealed with gaskets and stack is compressed between end plates. Bipolar plates also provide connection between inlet and outlet manifolds for hydrogen and oxygen supply and exhaust.

The performance of PEMFC is characterized by the Polarization curve shown in Fig. 1.2, where
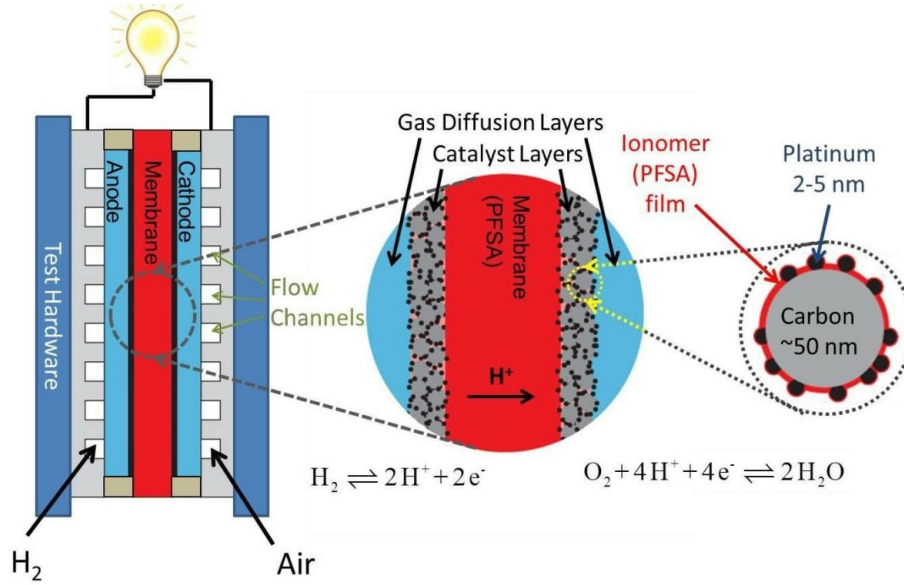
Figure 1.1: schematic of PEMFC [2]

the potential of the cell is plotted as a function of current density under the steady state operating condition. Three types of potential losses occur in a fuel cell : Activation losses, Ohmic losses and Mass transfer losses. The activation losses are due to the kinetics associated with the HOR and ORR reaction rates. The HOR is very fast on the catalyst in the anode side and hence the activation losses are small. The main contribution to the activation loss is at the cathode. The ORR overpotential is described by the Tafel equation.

$$\eta = bln\frac{i}{i_o} \tag{1.4}$$

where η is overpotetial, b is the Tafel slope and i_o is the exchange current density, which represents the reaction rate at zero overpotential.

The ohmic losses is caused by electronic and ionic conduction resistance,

$$\eta = IR \tag{1.5}$$

The ohmic losses are mainly due protonic conduction in the membrane and catalyst layer, electronic conduction in catalyst layer, gas diffusion layer, bipolar plates, current collector, also in contact resistance between the layers and the transfer of protons in ionomer of catalyst layer. As given by the above equation, ohmic losses vary linearly with current density. In the polarization curve, they are dominant for medium current withdrawal where a linear relation can be noticed.
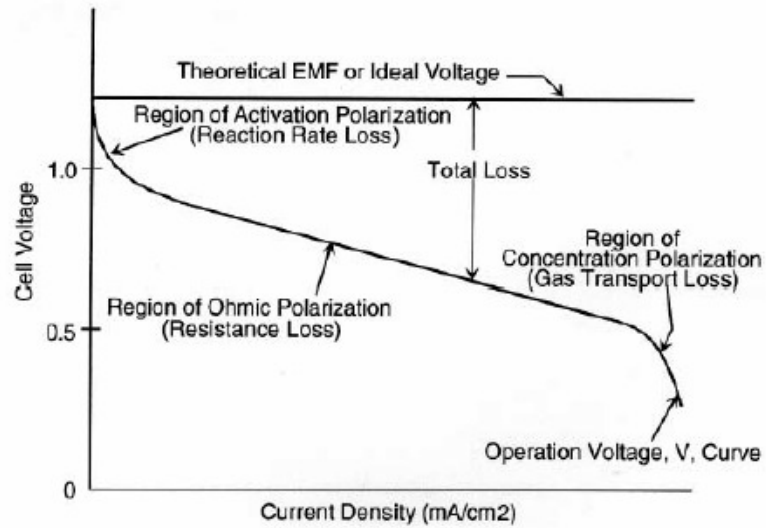
3

Figure 1.2: Polarization curve of fuel cell [3]

The mass transfer losses are due to oxygen transport by diffusion through the pores in GDL and catalyst layer. The losses are higher when the pores are blocked by water. As can be observed from the polarization curve, these losses are large at high current density.

Chapter 2

Literature Review

The performance of PEMFC in terms of kinetic, ohmic and mass transport overpotentials is qualitatively described in first chapter. In this chapter, the literature review of PEMFC modeling is given.

2.1 Membrane

The most used membrane for PEMFC is Perfluorosulfonic acid, also called as Dupont's Nafion. It's chemical structure shown in Fig. 2.1. The membrane consists of Perfluoroethersulfonic acid chains which are bonded with a Polytetratluoroehthylene (PTFE, Teflon) backbone to ensure mechanical strength. Each chain consists of SO^{3-} anionic groups. The sulfonate anions need cations to balance the charge. The sulfonate ions are hydrophilic whereas the backbone (Teflon) is a hydrophobic. Water content through the membrane varies as a result of the proton drag from the anode to the cathode side, a process called as Electroosmotic drag. The back diffusion of water from cathode side to anode due to concentration differences. The water content in the membrane is defined as the ratio of the number of water molecules to the number of charge $SO^{3-}H^+$ sites. The water content determines the proton conductivity of the membrane. The water content of the membrane is maintained by humidified inlet gases.

The water distribution and proton transport in the PEM Fuel Cell has been modeled by different methods. The first approach to modeling of Polymer Electrolyte Membrane is by Springer [5]. In this approach, the authors used dilute solution theory where the interaction of minor species and solvent are considered. Fuller and Newman [6] used concentration solution theory in which the interaction of all of the species in Polymer electrolyte are considered as significant and Fick's Law
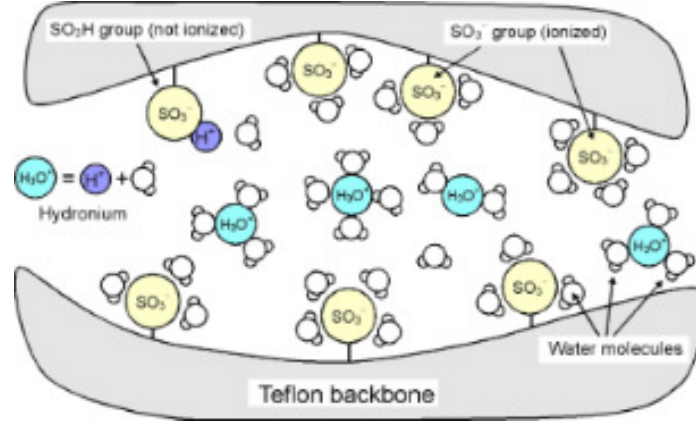
Figure 2.1: Structure of Nafion Membrane [4]

is replaced with equation of multicomponent diffusion.

The third approach is a hydraulic mathematical model for an ion-exchange membrane attached to gas-fed porous electrode of polymer electrolyte fuel cell by Bernardi and Verbrugge[7, 8].The driving forces for water transport depend on the hydraulic pressure and electro-osmotic drag. The main parameters in this model are electro kinetic permeability, hydraulic permeability, viscosity and conductivity.

2.2   Gas diffusion layer

The gas diffusion layer (Fig. 3.2) is made of carbon cloth or carbon paper. The main function of GDL is to provide a pathway for gas diffusion from flow channel to catalyst layer and to remove the water produced from catalyst layer interface. The GDL includes a micro-porous layer on catalyst layer side which is prepared with carbon black and PTFE.

The diffusion of gases inside the GDL is described by Stefan maxwell diffusion equations [6, 10, 11, 7, 8].

$$\frac{\nabla \mu_i}{RT} = \nabla \ln a_i = \sum_{j=1 j \neq i}^{n} \frac{x_i x_j}{D_{ij}} (v_j - v_i) = \sum_{j=1 j \neq i}^{n} \frac{c_i c_j}{c^2 D_{ij}} \left(\frac{N_j}{c_j} - \frac{N_i}{c_i} \right) \qquad (2.1)$$

In GDL, the mean free path of the gas molecules is low and pore diameter is high so molecular diffusion is dominant and hence the Stefan-Maxwell equations can be applied. In the catalyst layer the mean free path of the gas molecules is high compared to the pore diameter and hence Knudsen
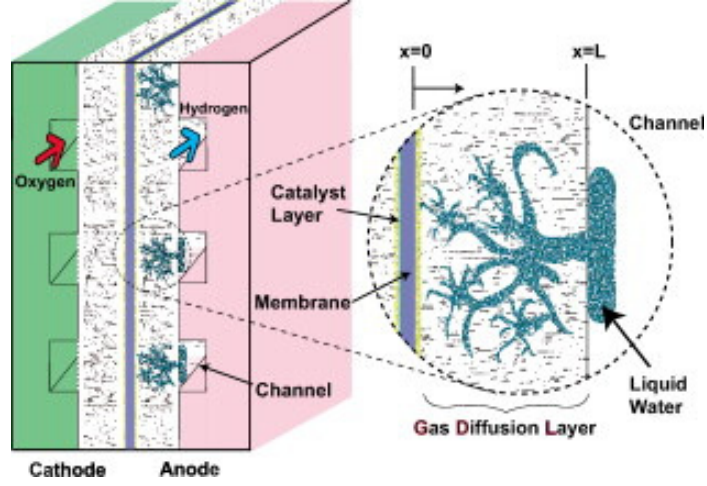
Figure 2.2: Gas diffusion layer [9]

diffusion is more dominant. In this case, an additional term is included in the above equation,

$$\frac{\nabla x_i}{RT} = \sum_{J=i} \frac{x_i N_j - x_j N_i}{PD_{ij}^{eff}} - \frac{N_i}{PD_{k_i}^{eff}} \tag{2.2}$$

were D_{eff} is the Knudsen diffusivity in between molecule aand the wall. Kulikovsky[12] and Wohr [13]are use such Knusdsen diffusion included models.

Gas Diffusion Layer is modelled assuming homogeneous cylindrical pores and by considering condensation and evaporation by M.Wohr and Bolwin[13]. The gas transport with in the pores is described by the dusty gas model combining Stefan Maxwell and Knudsen diffusions with convective transport by a pressure gradient. In [14] the gas diffusion layer is governed by a system of differential equations of material and energy balance for gases and water transport.

2.3   Catalyst layer

The catalyst layer is made of nano sized platinum particles supported on fine carbon grains, an electrolyte network of perflourosulfonate ionomer (PFSI) soaked with water and Teflon as a binder and a hydrophobizing agent. The carbon grains form agglomerates of larger sizes thereby creating pores of small and large sizes. The oxygen reduction reaction occurs on the catalyst sites adjacent to the ionomer phase in the larger gas pores Fig. 2.3.

The diffusion in the catalyst layer can occur in two ways: Molecular and Knudsen diffusions. The molecular diffusion occurs in the larger pores of the agglomerates while the Knudsen diffusion occurs in the primary pores of the carbon matrix.
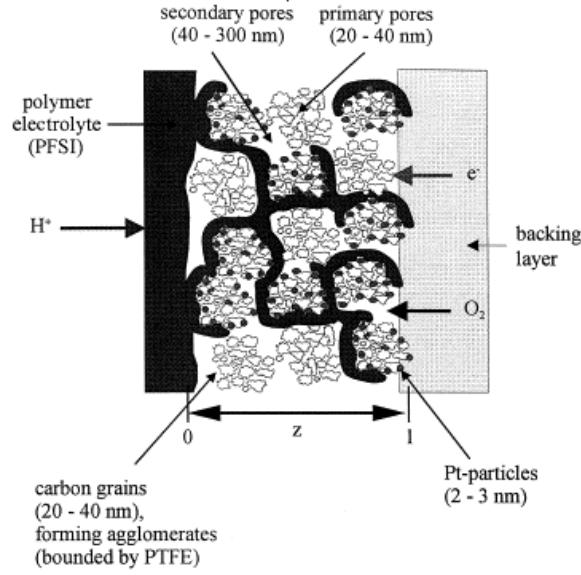
Figure 2.3: Catalyst layer Agglomerate model [19]

The first catalyst layer model was developed by springer[5] the electrochemical reaction described by the Tafel expression without adding loss in the cathode. The Fick's law diffusion considered in the ionomer of catalyst layer of Flooding model by Springer and Wilson[15].In this model consider the losses by the interfacial kinetics between the Pt and ionomer interface,gas and ionic transport limitation consider in cathode catalyst layer. Bernerdi and verbergge[7, 8] using the continuity equation for both oxygen depletion and water transport in the active catalyst layer described. Fuller and Newman[10, 11] expressed the Stefan maxwell equation used for the reactant transport in the catalyst layer pores. The effective diffusivity used for transport of reactants assumed in the fuel cell[16, 17, 18] by the Bruggeman Power law.

The diffusion of oxygen in ionomer pahse is described by Ridge et al[20]. The model describe the diffusion and reaction of oxygen and hydrogen ions in the active catalyst layer. The oxygen reduction reaction kinetics expressed by a Tafel equation[5, 6, 10, 21].

$$i = i_o \frac{p_{o2}}{p_{ref}} exp(\frac{\eta}{b}) \tag{2.3}$$

Here i_o is ion exchange current density, η is over potential and b is Tafel slope,which is often reported as mv/decade. many researcher have done on an approximately double slope for ORR at low potentials[22, 23, 24, 25].

8

Chapter 3

Characterization of Polymer Electrolyte fuel cell using AC Impedance Spectroscopy

3.1 Introduction

In a Polymer Electrolyte Membrane Fuel cell, air, hydrogen are sent to the cathode and anode sides. On both sides, the reactants are saturated with water vapor. In this chapter, the impedance modeling of the gas diffusion layer on the cathode side studied by [18] is presented along with the simulation results. In the cathode side, the transport of the three components, oxygen, nitrogen and water vapor in the gas diffusion layer is studied using the steady state Stefan-Maxwell equations. The steady state oxgyen concentration varies along the length of the gas diffusion layer. The steady state current is perturbed and the change in the oxygen concentration at the gas diffusion/catalyst layer interface is obtained.

3.2 Model of Backing Layer of Cathode Side

The model has three main assumptions. i) water vapor concentration is constant throughout the backing layer, ii) Nitrogen flux at steady state throughout the backing layer is zero and iii) Nitrogen flux at the interface between the gas diffusion layer and catalyst layer is zero even during the dynamics. The concentration of O_2, N_2 varies with the length along the gas diffution layer. The
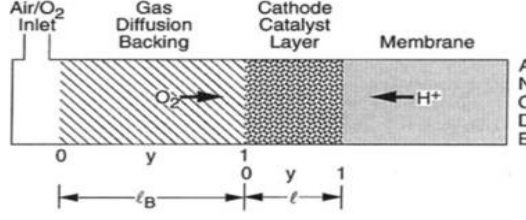
Figure 3.1: Schematic of PEMFC for modeling [18]

instantaneous current density is denoted by I. The steady state Stefan Maxwell multicomponent diffusion equation (Eq. 3.1) relate the instantaneous gradient in mole fraction of O_2 and water vapor to the O_2 and water vapor fluxes, N_o and N_w and their mole fractions x and w in Eqs. 3.2, 3.3.

$$\frac{\nabla \mu_i}{RT} = \nabla \ln a_i = \sum_{j=1j\neq i}^{n} \frac{x_i x_j}{D_{ij}}(v_j - v_i) = \sum_{j=1j\neq i}^{n} \frac{c_i c_j}{c^2 D_{ij}}\left(\frac{N_j}{c_j} - \frac{N_i}{c_i}\right) \tag{3.1}$$

The activity is chosen as the mole fraction assuming ideal gas conditions. The logarithm is also approximated as $\ln(x) = x - 1$ for moderate values of x.

$$\frac{dx}{dy} = [\alpha_o(xN_w - wN_o) + (xN_N - (1 - x - w)N_o)]\frac{l_B}{D_{eON}c} \tag{3.2}$$

$$\frac{dw}{dy} = [\alpha_o(wN_o - xN_w) + \alpha_N(wN_N - (1 - x - w)N_w)]\frac{l_B}{D_{eON}c} = 0 \tag{3.3}$$

The last equation is equal to zero due to the first assumption.

$$D_{eoN} = \frac{\epsilon_B}{\tau}\frac{D_{soN}}{P_a}\left(\frac{T_S}{T}\right)^{1.823}, \qquad c = \frac{1}{V_M}\frac{P_a}{P_S}\frac{T_S}{T}, \qquad \alpha_N = \frac{D_{soN}}{D_{swN}}, \qquad \alpha_o = \frac{D_{soN}}{D_{sow}}$$

where D_{eoN} is the effective diffusivity while D_{soN} is the diffusivity at standard conditions which are considered as 1 atm and 0° celcius. It was assumed in [18] that the sum of the O_2 and N_2 fluxes equals $\frac{I}{4F}$. Using this fact and

$$\alpha_o(wN_o - xN_w) + \alpha_N(wN_N - (1 - x - w)N_w) = 0$$

we obtain,

$$N_w = \frac{wN_w + \frac{\alpha_o}{\alpha_N}w(\frac{I}{4F} - N_N)}{1 - w + (\frac{\alpha_O}{\alpha_N} - 1)x}$$

By using the above result and Eq. 3.2, the nitrogen flux can be obtained.

$$N_N = \frac{1}{K}\frac{1}{\beta_1}\left[G(x)\frac{dx}{dy} + (\beta_1 - x)\frac{I}{I_B}\right]$$

where, $\beta_1 = 1 - w$, $\beta_2 = \frac{\alpha_o}{\alpha_N} - 1$, $\beta_3 = 1 - w + \alpha_o w$, $\alpha_o w = \beta_3 - \beta_1$, $I_B = \frac{4FCD_{eoN}}{l_B}$, $K = \frac{l_B}{D_{eoN}C}$ and $G(x) = \frac{\beta_1 + \beta_2 x}{\beta_3 + \beta_2 x}$.

Using the assumption that at steady state the nitrogen flux equals zero, we obtain

$$\frac{I}{I_B}(\beta_1 - x) = -G(x)\left(\frac{dx}{dy}\right)$$

Integrating the above equation results in the following,

$$\frac{I}{I_B}\left(\int_{y=0}^{y=1} dy\right) = -\int_{x(0)}^{x(1)} \frac{G(x)}{(\beta_1 - x)}dx$$

This results in

$$\frac{I}{I_B}y = \beta_4 \log\left(\frac{\beta_3 + \beta_2 x(1)}{\beta_3 + \beta_2 x(0)}\right) + \beta_5 \log\left(\frac{\beta_1 - x(1)}{\beta_1 - x(0)}\right) \tag{3.4}$$

where

$$\beta_4 = \frac{(\beta_1 - \beta_3)}{(\beta_2\beta_1 + \beta_3)} \quad and \quad \beta_5 = \beta_1\frac{\beta_2 + 1}{\beta_2\beta_1 + \beta_3}$$

Eq. 3.4 represents the dependance of oxygen mole fraction on the current density and fractional distance through the gas diffusion layer.

In the dynamic case, the continuity equation applied on oxygen in the gas diffusion layer results in $C\epsilon_B\frac{\partial x}{\partial t} = -\frac{1}{l_B}\frac{\partial N_o}{\partial y}$. Since, $N_o + N_N = \frac{I}{4F}$ and I is assumed to te indepedent of y, we obtain,

$$C\epsilon_B\frac{\partial(\delta x)}{\partial t} = -\frac{1}{l_B}\frac{\partial\delta N_o}{\partial y} = \frac{1}{l_B}\frac{\partial(\delta N_N)}{\partial y}$$

where $\delta x, \delta N_o, \delta N_N$ represent perturbations. Therefore,

$$\begin{aligned}
\frac{\beta_1 l_B}{CD_{eoN}}\frac{d(\delta N_N)}{dy} = \frac{\beta_1}{\omega_B}\frac{\partial(\delta x)}{\partial t} &= \frac{d}{dy}\left[\delta\left(\frac{I}{I_B}(\beta_1 - x)) + G(x)\frac{dx}{dy}\right)\right] \\
&= \frac{d}{dy}\left[\frac{\delta I}{I_B}(\beta_1 - x) - \frac{I}{I_B}\delta x + G(x)\delta(\frac{dx}{dy}) + \frac{dG}{dx}\frac{dx}{dy}\delta x\right] \\
&= \left[\frac{\delta I}{I_B}\left(-\frac{dx}{dy}\right) - \frac{I}{I_B}\frac{d\delta x}{dy} + \frac{dG}{dx}\frac{dx}{dy}\frac{d(\delta x)}{dy}G(x)\frac{d^2(\delta x)}{dy^2}\right] \\
&\quad + \left[\frac{d^2 G}{dx^2}\left(\frac{dx}{dy}\right)^2\delta x + \left(\frac{dG}{dx}\right)\left(\frac{d^2 x}{dy^2}\right)\delta x + \frac{dG}{dx}\frac{dx}{dy}\frac{d(\delta x)}{dy}\right]
\end{aligned} \tag{3.5}$$

11

where $\omega_B = \frac{D_{eoN}}{l_B^2} = \frac{D_{soN}}{\tau P_a l_B^2} \left(\frac{T}{T_S} \right)^{1.823}$, $C = \frac{1}{V_m} \frac{P_a}{P_s} \frac{T_S}{T}$, $D_{eoN} = \frac{\epsilon_B}{\tau} \frac{D_{soN}}{P_a} (\frac{T}{T_s})^{1.823}$.

The Laplace transformed variables are denoted with an overbar as follows.

$$L(\delta x) = \bar{x}(y, s) \qquad L((\delta I)) = \bar{I}(s)$$

$$L \left(\frac{d(\delta(x))}{dy} \right) = \bar{x}'(y, s) \qquad L \left(\frac{d(\delta x)}{dy^2} \right) = \bar{x}''(y, s)$$

After applying Laplace transform on Eq. 3.5 we get the following frequency dependent differential equation.

$$G(x)\bar{x}''(y, s) + \left(2\frac{dG}{dx}\frac{dx}{dy} - \frac{I}{I_B} \right) \bar{x}'(y, s) + \left(\frac{d^2 G}{dx^2}(\frac{dx}{dy})^2 + \frac{dG}{dx}\frac{d^2 x}{dy^2}\frac{\beta_1 s}{w_B} \right) \bar{x}(y, s) = \frac{dx}{dy}\frac{\bar{I}(s)}{I_B}$$

along with the boundary conditions,

1. $\bar{x}(0, s) = 0$

2. $\delta N_N(s)|_{y=1} = 0 = \frac{\bar{I}(s)}{I_B} [\beta_1 - \bar{x}(1)] + G|_{x(1)}\bar{x}'(1, s) + \left[\frac{dG}{dx}|_{x(1)}\frac{dx}{dy}|_{x(1)} - \frac{I}{I_B} \right] \bar{x}(1, s) = 0$

where $I(s) = \frac{\omega}{s^2+\omega^2}$ for sinusoidal perturbation in the current and the second boundary condition is obtained from Eq. 3.5 at $y = 1$. Finally, the impedance is calculated via

$$z = \frac{P_a * \bar{x}(1, s)}{\bar{I}(s)} \tag{3.6}$$

3.3   Impedance of Gas Diffusion Layer

The impedance at interface of GDL and catalyst layer $z = \frac{P_a * \bar{x}(1,s)}{\bar{I}(s)}$ shown in Fig. 3.2. The high frequencies are towards the left and the low frequencies are towards the right as shown in the figure. The impedance as a function of different ambient pressures are observed. At higher frequencies a straight line limit can be observed. On the other side of the spectrum, for zero frequency, the resistivity can be determined.
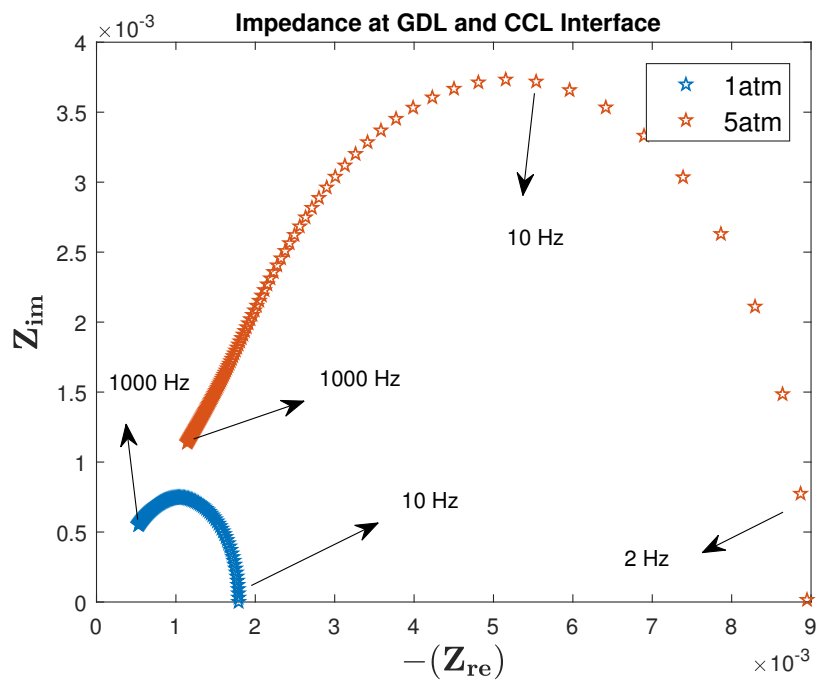
Figure 3.2: Impedance of Gas diffusion Layer

Chapter 4

Physical Model of Cathode Catalyst Layer

4.1 Introduction

The previous chapter described the impedance of the gas diffussion layer in terms of change of oxygen concentration at the catalyst layer interface with respect to the current perturbation. In this chapter, the impedance of the cathode catalyst (CCL) layer is studied. The performance of the fuel cell is determined mainly by the CCL where the ionic and electronic currents are converted to flux of water.

The schematic of cathode catalyst layer thickness is shown in Fig. 4.2. The flux of protons decreases from electrolyte — catalyst layer interface to the catalyst — gas diffusion layer interface. The flux of electrons decrease from GDL (gas diffusion layer) interface to the membrane interface.The reactants (oxygen) decrease from right hand side to left hand side due to the Oxygen Reduction Reaction (ORR).

The chapter discusses the the complete macro homogeneous model of fuel cell catalyst layer impedance by A. A. Kulikovsky [27]. This approach considers the non-stationary model of CCL performance based on Perry-Neuman-Cairns model with butler-volmer conversion function. The model equations are linearized and converted frequency domain and an exact analytical solution to the system equations is obtained in the case of small cell current. For high cell currents, an approximate solution is obtained.
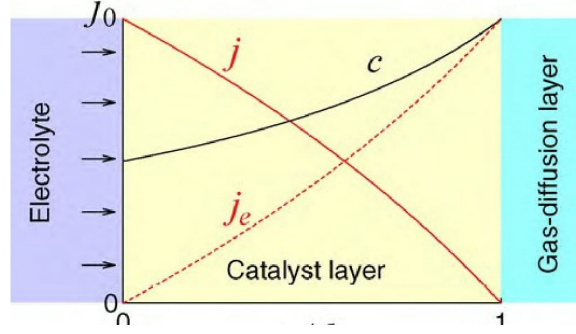
Figure 4.1: Schematic of Cathode catalyst layer [26]

4.2 The Butler-Volmer Equation

The Butler-Volmer equation relates the current density S to the loss in Galvanic potential called as activation overpotential η.

$$S = i_* \left[\exp\left(\frac{\alpha F \eta}{RT} \right) - \exp\left(\frac{-(1-\alpha)F\eta}{RT} \right) \right]$$

where i_* is volumetric exchange current density (A/cm^3) and α is the transfer co efficient which describes the shape of the energy barrier between initial and final states of reaction. For a symmetric barrier with $\alpha = 0.5$, we obtain

$$S = i_* \left[\exp\left(\frac{\eta}{b} \right) - \exp\left(\frac{-\eta}{b} \right) \right]$$
$$= 2i_* \sinh\left(\frac{\eta}{b} \right)$$

where $b = \frac{RT}{\alpha F}$ is called the Tafel slope.

4.3 The Model

The unsteady model of the cathode catalyst layer can be described by the following equations.

$$C_{dl} \frac{\partial \eta}{\partial t} + \frac{\partial j}{\partial x} = -2i_* \sinh\left(\frac{\eta}{b} \right)$$
$$j = -\sigma_t \frac{\partial \eta}{\partial x}$$
$$\frac{\partial c}{\partial t} - D\frac{\partial^2 c}{\partial x^2} = -\frac{2i_*}{nF}\left(\frac{c}{c_{ref}} \right) \sinh\left(\frac{\eta}{b} \right)$$

where C_{dl} is the double layer capacitance(F/cm^3), η is the half cell over-potential, j is the local proton current density, x is the distance from the membrane , i_* is volumetric exchange current density (Acm^{-3}), c is the local concentration of oxygen , c_{ref} is the reference inlet concentration, σ_t is the CCL proton conductivity and D is the effective diffusion co-efficient of oxygen in the catalyst layer.

Physically oxygen diffusion in the CCL is due to free molecular diffusion in large pores and due to knudsen diffusion in small pores. The action of both mechanisms is described by simple Fick's formula with average effective diffusion coefficient.

The over-potential is given by $\eta = \phi_m - \phi_c + E_{eq}$, where ϕ_c, ϕ_m, E_{eq} are carbon phase, membrane phase and equilibrium potentials respectively. The conductivity of carbon phase is very large and hence the gradient of ϕ_c can be neglected. Therefore, $\nabla \phi_m \approx \nabla \eta$.

The first model equation represents the decaying of ionic current density towards the GDL due to charging of double layer and proton conversion due to the ORR. The second model equation is the Ohm's Law relating the proton current density to gradient of over potential. The last equation represents the oxygen mass conservation equation.

Using dimension less variables,

$$\bar{x} = \frac{x}{l_t}, \bar{t} = \frac{t}{t_*}, \bar{\eta} = \frac{\eta}{b}, \bar{j} = \frac{j}{j_*}, \bar{D} = \frac{D}{D_*}, \bar{Z} = \frac{Z\sigma_t}{l_t}, \bar{c} = \frac{c}{c_{ref}}$$

where

$$t_* = \frac{C_{dl}b}{2i_*}, j_* = \frac{\sigma_t b}{l_t}, D_* = \frac{\sigma_t b}{nFc_{ref}}$$

the model equations translate into,

$$\frac{\partial \bar{\eta}}{\partial t} + \epsilon^2 \frac{\partial \bar{j}}{\partial \bar{x}} = -\bar{c}\sinh(\bar{\eta})$$
$$\bar{j} = -\frac{\partial \bar{\eta}}{\partial \bar{x}} \quad (4.1)$$
$$\mu^2 \frac{\partial \bar{c}}{\partial \bar{t}} - \epsilon^2 \bar{D} \frac{\partial^2 \bar{c}}{\partial \bar{x}^2} = -\bar{c}\sinh(\bar{\eta})$$

where $\epsilon = \sqrt{\frac{\sigma_t b}{2i_* l_t^2}}$ is the Newman's reaction penetration depth and $\mu^2 = \frac{nFc_{ref}}{c_{dl}b}$.

Let $\bar{\eta}^0$ and $\bar{c}^0$ be the steady state solution to Eq. 4.1. Using the perturbations,

$$\bar{\eta} = \bar{\eta}^0 + \bar{\eta}^1 \exp(i\bar{\omega}\bar{t})$$
$$\bar{c} = \bar{c}^0 + \bar{c}^1 \exp(i\bar{\omega}\bar{t})$$

and neglecting the products of disturbance terms and subtracting the steady state equations for $\bar{\eta}^0$ and $\bar{c}^0$, the following differential equations and boundary conditions are obtained.

$$\epsilon^2 \frac{\partial^2 \bar{\eta}^1}{\partial \bar{x}^2} = \sinh(\bar{\eta}^0)\bar{c}^1 + (\bar{c}^0 \cosh \bar{\eta}^0 + i\bar{\omega})\bar{\eta}^1$$

$$\epsilon^2 \bar{D} \frac{\partial^2 \bar{c}^1}{\partial^2 \bar{x}^2} = (\sinh \bar{\eta}^0 + i\bar{\omega}^0 \mu^2)\bar{c}^1 + \bar{c}^0 \cosh(\bar{\eta}^0)\bar{\eta}^1$$

(4.2)

$$\bar{\eta}^1(1) = \bar{\eta}^1_1, \qquad \frac{\partial \bar{\eta}^1}{\partial \bar{x}}\big|_1 = 0$$

$$\frac{\partial \bar{c}^1}{\partial \bar{x}}\big|_0 = 0, \qquad \bar{c}^1(1) = 0$$

4.4   Ideal Oxygen Transport

For ideal oxygen transport, it is assumed that $\bar{c}^0 = 1$ and $\bar{c}^0 = 1$ in Eq. 4.2, i.e.,1) the steady state oxygen concentration in CCL does not depend on the spatial and the temporal dimensions and 2) the perturbations in oxygen concentration are zero. Then, the previous equation reduces to,

$$\epsilon^2 \frac{\partial^2 \bar{\eta}^1}{\partial \bar{x}^2} = (\cosh \bar{\eta}^0 + i\bar{\omega})\bar{\eta}^1$$

If the cell current is small, $\bar{\eta}^0 \ll 1$ and is almost independent of $\bar{x}$. From the previous equation, we obtain,

$$\epsilon^2 \frac{\partial^2 \bar{\eta}^1}{\partial \bar{x}^2} = (1 + i\bar{\omega})\bar{\eta}^1$$

Solving this equation with the boundary conditions (Eq. 4.2), the following expression for the perturbed overpotential can be obtained

$$\frac{\bar{\eta}^1}{\bar{\eta}^1_1} = \cos(\phi(1 - \bar{x}))\bar{\eta}^1$$

(4.3)

where $\phi = \sqrt{\frac{-1 - i\bar{\omega}}{\epsilon^2}}$

Differentiating the above equation with respect to $\bar{x}$ we get the perturbation in cell current .

$$\frac{\bar{j}^1}{\bar{\eta}^1_1} = -\phi \sin(\phi(1 - \bar{x}))\bar{\eta}^1$$

(4.4)

To calculate the impedance at the membrane — catalyst interface, we set $\bar{x} = 0$ and calculate

the ratio of Eq. 4.3 and Eq. 4.4.

$$\bar{z} = \frac{\bar{\eta}^1}{\bar{j}^1} = -\frac{1}{\phi \tan \phi}$$

The real and imaginary parts of the above expression can be calculated.

$$\bar{z}_{re} = \frac{\epsilon^2}{\sqrt{1+\bar{\omega}^2}} \left(\frac{\beta \sinh(2\beta) - \alpha \sin(2\alpha)}{\cosh(2\beta) - \cos(2\alpha)} \right)$$

$$\bar{z}_{im} = -\frac{\epsilon^2}{\sqrt{1+\bar{\omega}^2}} \left(\frac{\beta \sin(2\alpha) + \alpha \sinh(2\beta)}{\cosh(2\beta) - \cos(2\alpha)} \right)$$

where $\alpha = \sqrt{\frac{\sqrt{1+\bar{\omega}^2}-1}{2\epsilon^2}}$ $\qquad$ $\beta = \sqrt{\frac{\sqrt{1+\bar{\omega}^2}+1}{2\epsilon^2}}$

4.5 Impedance of Cathode Catalyst Layer

The impedance for ideal oxygen transport in the cathode catalyst layer is shown in Fig-4.2. The high frequency values are to the left (near the zeros of the axes) of the plot whereas the low frequency ones are to the right. The impedance depends on the Newman's reaction penetration depth ϵ. When the penetration depth is high ($\epsilon = 1000$), a semicircle is obtained. For high frequencies, a straight line can be observed from the impedance plot. The slope of this line is 45°. For the impedance at reaction depth $\epsilon = 1$, this line is clearly visible. The impedance for the high frequencies can be approximated as $\frac{\epsilon}{\sqrt{2\bar{\omega}}}(1-j)$. For $\bar{\omega} = 0$, we obtain the resistivity of the CCL. Note that for $\bar{\omega} = 0$, $\bar{z}_{im} = 0$ whereas $\bar{z}_{re} = \frac{\epsilon \sinh(2/\epsilon)}{\cosh(2/\epsilon)-1}$.
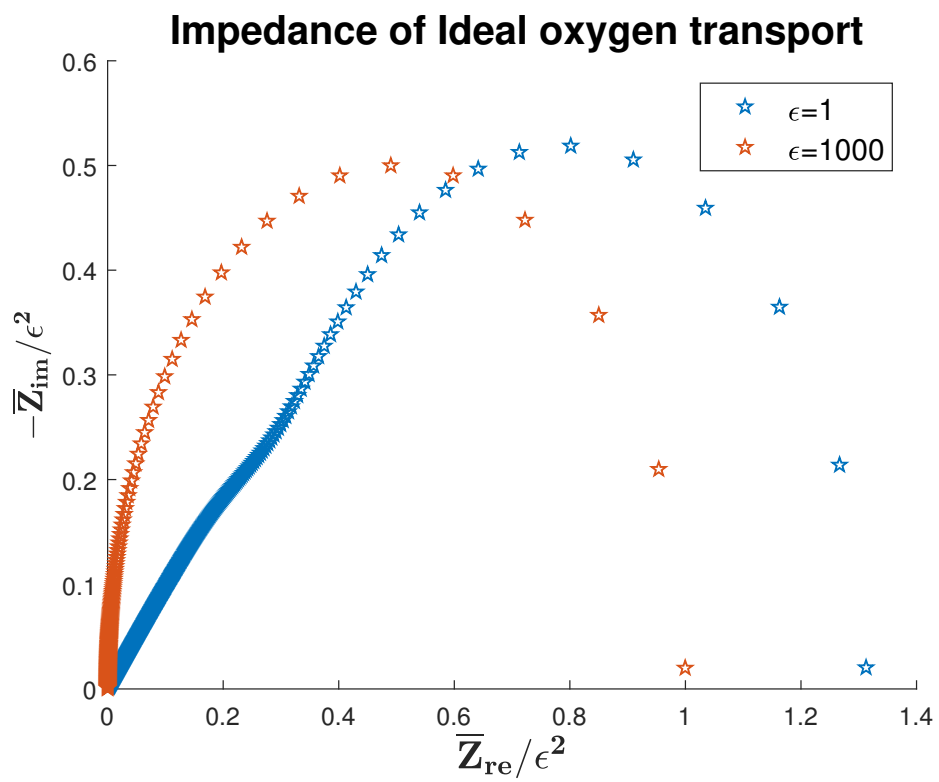
Figure 4.2: Impedance of the CCL

References

[1] M. L. Perry and T. F. Fuller. A historical perspective of fuel cell technology in the 20th century. *Journal of the electrochemical society* 149, (2002) S59–S67.

[2] B. P. Setzler, A. Dabonot, and T. Fuller. Determination of Electroosmotic Drag and Proton Conduction Mechanism In Proton Exchange Membranes for Use In Low Temperature PEMFCs. In AIChE Annual Meeting, Minneapolis, MN. 2011 .

[3] X. Huang, Z. Zhang, and J. Jiang. Fuel Cell Technology for Distributed Generation: An Overview 2, (2006) 1613 – 1618.

[4] R. Zeis. Materials and characterization techniques for high-temperature polymer electrolyte membrane fuel cells. *Beilstein journal of nanotechnology* 6, (2015) 68.

[5] T. E. Springer, T. Zawodzinski, and S. Gottesfeld. Polymer electrolyte fuel cell model. *Journal of the electrochemical society* 138, (1991) 2334–2342.

[6] T. F. Fuller. Solid-polymer-electrolyte fuel cells. Technical Report, Lawrence Berkeley Lab., CA (United States) 1992.

[7] D. M. Bernardi and M. W. Verbrugge. Mathematical model of a gas diffusion electrode bonded to a polymer electrolyte. *AIChE journal* 37, (1991) 1151–1163.

[8] D. M. Bernardi and M. W. Verbrugge. A mathematical model of the solid-polymer-electrolyte fuel cell. *Journal of the Electrochemical Society* 139, (1992) 2477–2491.

[9] B. A. McCain, A. G. Stefanopoulou, and J. B. Siegel. Controllability and observability analysis of the liquid water distribution inside the gas diffusion layer of a unit fuel cell model. *Journal of Dynamic Systems, Measurement, and Control* 132, (2010) 061,303.

[10] T. F. Fuller and J. Newman. Water and thermal management in solid-polymer-electrolyte fuel cells. *Journal of the Electrochemical Society* 140, (1993) 1218–1225.

[11] T. F. Fuller and J. Newman. Experimental determination of the transport number of water in Nafion 117 membrane. *Journal of The Electrochemical Society* 139, (1992) 1332–1337.

[12] A. Kulikovsky, J. Divisek, and A. Kornyshev. Modeling the cathode compartment of polymer electrolyte fuel cells: dead and active reaction zones. *Journal of the Electrochemical Society* 146, (1999) 3981–3991.

[13] M. Wöhr, K. Bolwin, W. Schnurnberger, M. Fischer, W. Neubrand, and G. Eigenberger. Dynamic modelling and simulation of a polymer membrane fuel cell including mass transport limitation. *International Journal of Hydrogen Energy* 23, (1998) 213–218.

[14] D. Bevers, M. Wo, K. Yasuda, K. Oguro et al. Simulation of a polymer electrolyte fuel cell electrode. *Journal of Applied Electrochemistry* 27, (1997) 1254–1264.

[15] T. E. Springer, M. S. Wilson, and S. Gottesfeld. Modeling and experimental diagnostics in polymer electrolyte fuel cells. *Journal of the Electrochemical Society* 140, (1993) 3513–3526.

[16] N. Zamel and X. Li. Effective transport properties for polymer electrolyte membrane fuel cells–with a focus on the gas diffusion layer. *Progress in energy and combustion science* 39, (2013) 111–146.

[17] R. Barbosa, J. Andaverde, B. Escobar, and U. Cano. Stochastic reconstruction and a scaling method to determine effective transport coefficients of a proton exchange membrane fuel cell catalyst layer. *Journal of Power Sources* 196, (2011) 1248–1257.

[18] T. Springer, T. Zawodzinski, M. Wilson, and S. Gottesfeld. Characterization of polymer electrolyte fuel cells using AC impedance spectroscopy. *Journal of the Electrochemical Society* 143, (1996) 587–599.

[19] M. Eikerling and A. Kornyshev. Modelling the performance of the cathode catalyst layer of polymer electrolyte fuel cells. *Journal of Electroanalytical Chemistry* 453, (1998) 89–106.

[20] S. Ridge, R. E. White, Y. Tsou, R. Beaver, and G. Eisman. Oxygen reduction in a proton exchange membrane test cell. *Journal of the Electrochemical Society* 136, (1989) 1902–1909.

[21] A. Z. Weber and J. Newman. Transport in polymer-electrolyte membranes III. Model validation in a simple fuel-cell model. *Journal of the Electrochemical Society* 151, (2004) A326–A339.

[22] A. Parthasarathy, C. R. Martin, and S. Srinivasan. Investigations of the O 2 Reduction Reaction at the Platinum/Nafion® Interface Using a Solid-State Electrochemical Cell. *Journal of the Electrochemical Society* 138, (1991) 916–921.

[23] A. Parthasarathy, S. Srinivasan, A. J. Appleby, and C. R. Martin. Temperature dependence of the electrode kinetics of oxygen reduction at the platinum/Nafion® interfacea microelectrode investigation. *Journal of the Electrochemical Society* 139, (1992) 2530–2537.

[24] A. Parthasarathy, S. Srinivasan, A. J. Appleby, and C. R. Martin. Pressure dependence of the oxygen reduction reaction at the platinum microelectrode/nafion interface: electrode kinetics and mass transport. *Journal of the Electrochemical Society* 139, (1992) 2856–2862.

[25] T. Lehtinen, G. Sundholm, S. Holmberg, F. Sundholm, P. Björnbom, and M. Bursell. Electrochemical characterization of PVDF-based proton conducting membranes for fuel cells. *Electrochimica Acta* 43, (1998) 1881–1890.

[26] A. Kulikovsky. The regimes of catalyst layer operation in a fuel cell. *Electrochimica acta* 55, (2010) 6391–6401.

[27] A. Kulikovsky. A physical model for catalyst layer impedance. *Journal of Electroanalytical Chemistry* 669, (2012) 28–34.